Application of Terahertz Synchrotron Radiation at UVSOR-II

Shin-ichi Kimura[*,†] and Takafumi Mizuno[†]

[*]*UVSOR Facility, Institute for Molecular Science, Okazaki 444-8585, Japan*
[†]*School of Physical Sciences, The Graduate University for Advanced Studies (SOKENDAI), Okazaki 444-8585, Japan*

Abstract. The infrared-terahertz beamline at UVSOR-II has been upgraded in 2004 for covering very low energy region below 0.3 THz (= 10 cm^{-1}). At the beamline, several characteristic experiments in the terahertz region are performed. Two examples of such experiments, reflectivity measurements at low temperatures and at high pressures are reported.

Keywords: Synchrotron radiation, Terahertz spectroscopy, Infrared
PACS: 41.60.Ap, 42.72.Ai, 78.30.-j, 78.68.+m

INTRODUCTION

Recently, electromagnetic waves in the terahertz region (THz) attract attention because it will become a new probing light source for non-destructive examinations in place of the x-ray. The THz light can also reveal the low energy excitation of materials, for instance, vibration modes of large molecules such as proteins, weak bonding between surfaces and adsorbed molecules, and the electrodynamics of quasiparticles of solids and so on. To study such basic sciences, the firstly dedicated infrared synchrotron radiation beamline (BL6A1) has been constructed at UVSOR about two decades ago [1] and so many scientific activities have been produced from the beamline. In 2003, UVSOR was upgraded to the lowest emittance ring (27 nm rad) among small SR's with the acceleration energy below 1 GeV and the name was also changed to UVSOR-II [2]. Simultaneously, BL6A1 was also upgraded to the new IR-THz beamline (BL6B) with high brilliance and high flux as shown in Fig. 1 [3]. To obtain the higher performance, we employed a so-called "magic mirror" with a large acceptance angle (215(H) $\times$ 80(V) $mrad^2$), which has been successfully installed at the infrared beamline of SPring-8 [4], for the first mirror [5]. The upgrading of the beamline gives us that the photon flux and brilliance of BL6B become four and 10^2 times larger than BL6A1, respectively. The spectral intensity in the THz region becomes very high as a Si bolometer saturates.

At the present, two permanent end stations are equipped at BL6B. One is the apparatus for reflection-absorption spectroscopy of solid samples with mm-size constructed two decades ago [1]. The apparatus can be removed and replaced to apparatuses brought by users, for instance, a magneto-optical apparatus [6] and an infrared reflection-absorption spectroscopy apparatus for adsorbed molecules [7]. The other is a THz microscope for the reflection and transmission spectroscopy of small samples with the diffraction-limit resolution [7]. The microscope covers down to 30 cm^{-1} (= 3.7 meV) that is lower wavenumber than that of a commercial infrared microscope because large Schwarzschild mirrors are employed. At an infrared beamline BL43IR of SPring-8, there is also a microscope which covers down to 100 cm^{-1} (= 12 meV) [8]. Since the brilliance in the THz region of BL6B of UVSOR-II is higher than that of BL43IR of SPring-8, the accessible lowest wavenumber of BL6B is lower. This is the advantage to investigate the electrodynamics of solids under pressures and other functionalities. These two permanent end stations are opened for users.

In this paper, we present two experimental results obtained by using the two permanent end stations at BL6B of UVSOR-II. One is the electromagnetic dynamics of strongly correlated insulator, SmB_6, at low temperature. The other is the insulator-metal transition of SmS under pressures using the THz microscope.

TERAHERTZ SPECTROSCOPY OF SMB_6 AT LOW TEMPERATURES

SmB_6, which is one of typical Kondo semiconductors, has been studied over two decades. In the previous studies, two different energy gap size were proposed, one is about 5 meV and the other about 15 meV [9]. However, a recent study using higher purity samples reveals that the lower energy absorption band originates from impurities because the lower energy absorption becomes small [10, 11]. The higher energy gap is concluded to be intrinsic and to originate from the hybridization between the localized Sm $4f$ state and the Sm $5d$ conduction

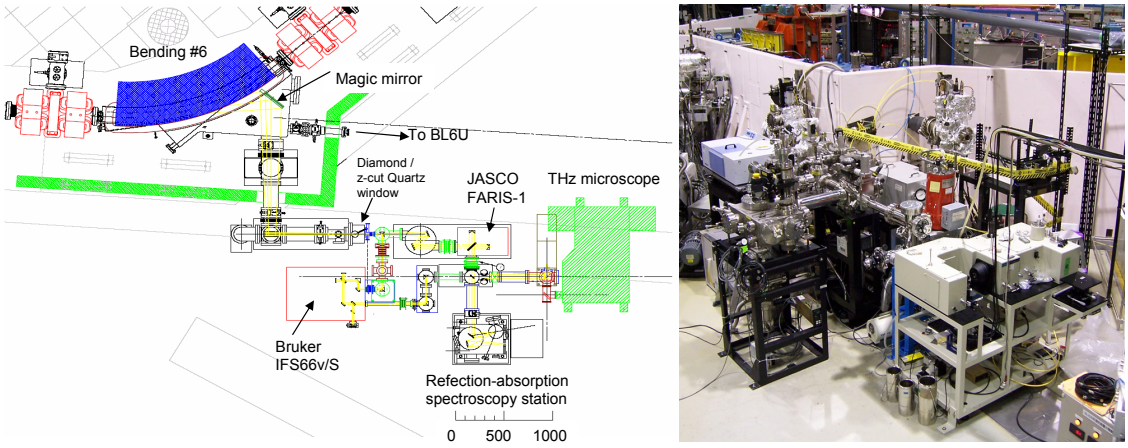

FIGURE 1. The top view (left) and the picture (right) of the infrared-terahertz beamline (BL6B) at UVSOR-II.

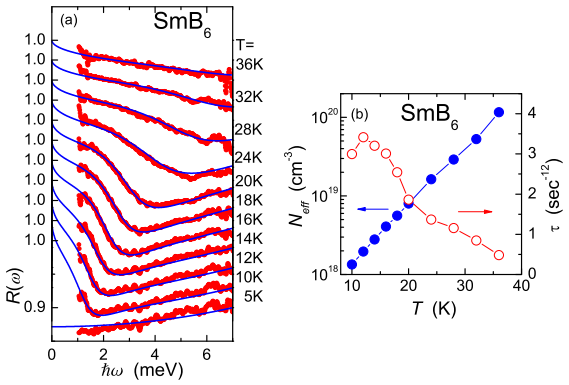

FIGURE 2. (a) Temperature dependence of reflectivity spectrum of SmB_6 in the THz region (thick lines) and fitting functions by the combination of a Drude and two Lorentz functions (thin lines). Successive curves are offset by 0.03 for clarity. (b) Obtained parameters of the effective electron number (N_{eff}) and the relaxation time (τ) of the Drude function as a function of temperature.

band, so-called cf–hybridization [12]. In the case of the cf–hybridization, a regid band model is suitable to explain the physical properties. However, the specific heat curve cannot be explained by a rigid band model [13]. This means that there is the temperature dependent parameters in the electronic structure as well as in the charge dynamics.

On the other hand, the magnetic excitation at 14 meV grows up with decreasing temperature below 20 K observed by a neutron inelastic scattering [14]. The magnetic excitation energy is similar to the energy gap observed in optical spectra. Therefore, if the cf–hybridization bands exist at the energy gap edge, the character of carriers should have the same temperature dependence. Optical reflection spectroscopy is one of good probes to investigate the character of carriers. In the SmB_6 case, the signal from the thermally excited carriers appears in the THz region. The change of the fitting parameters of the Drude function as a function of temperature must reflect the property at the energy gap edge. Then we measured the temperature dependence of the reflectivity spectrum in the THz region.

Figure 2(a) indicates the temperature dependence of reflectivity spectrum [$R(\omega)$] of SmB_6 by thick lines. At T =5 K, the reflectivity does not approach to unity with decreasing photon energy. This indicates the insulating character. With increasing temperature, the reflectivity grows up from the lower energy side. The high reflectivity originates from the Drude component due to thermally excited carriers. The Drude component indicates the electronic structure thermally excited area near the energy gap edge.

The fitted curve using one Drude and two Lorentz functions are indicated by thin solid lines in Fig. 2(a). The fitting function is as follows;

$$\hat{\varepsilon}(\omega) = \varepsilon_\infty - \frac{4\pi N_{eff} e^2}{m(\omega^2 - i\omega/\tau)} + \sum_{i=1}^{n} \frac{4\pi N_i e^2}{m\{(\omega_{i0}^2 - \omega^2) - i\omega/\tau_i\}}$$

$$R(\omega) = \left| \frac{1-\hat{\varepsilon}(\omega)^{1/2}}{1+\hat{\varepsilon}(\omega)^{1/2}} \right|^2$$

Here, $\hat{\varepsilon}(\omega)$, $\hat{n}(\omega)$ and $R(\omega)$ are a complex dielectric function, a complex refractive index and a reflectivity spectrum, respectively. ε_∞ is the sum of ε_1 above the measured energy region, N_{eff} and τ the effective number and the relaxation time of carriers, respectively, m the rest mass of an electron, N_i, ω_{i0} and τ_i are the intensity, resonance frequency and the relaxation time of i-th bound state including energy gaps of electronic structure and optical phonons, reflectivity. The two Lorentz functions were set to the main gap at 15 meV and to the impurity state at 5 meV. The fitting functions can reproduce

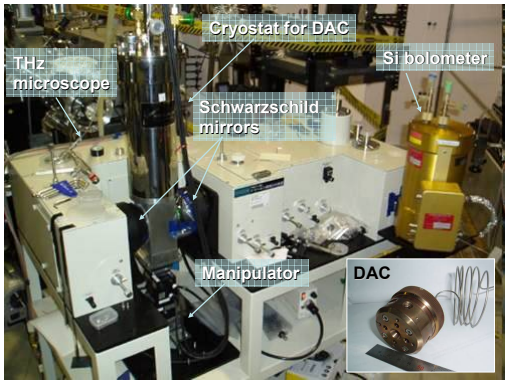

FIGURE 3. Photo of terahertz microscope with a high pressure diamond anvil cell (DAC) at BL6B of UVSOR-II.

the experimental curves well. The obtained N_{eff} and τ derived from the fitting parameters are shown as the function of temperature in Fig. 2(b). If an activation type behavior [$N_{eff} \propto \exp(-2\Delta/k_{\rm B}T)$, where Δ is the energy gap and $k_{\rm B}$ the Boltzmann constant] is expected, $\log N_{eff}$ should be proportional to $1/T$. However $\log N_{eff}$ is proportional to T as shown in Fig. 2(b). This indicates that the energy gap can not be explained by the rigid band model but it may indicate the energy gap shrinks with increasing temperature. Two-state model might be assumed to explain the behavior [15]. On the other hand, τ rapidly increases with decreasing temperature below 20 K. The temperature is coincident with that of the growth of the magnetic excitation at 14 meV [14]. This means that the thermally excited carriers strongly relates to the magnetic excitation at 14 meV.

TERAHERTZ SPECTROSCOPY OF SMS UNDER PRESSURES

The infrared synchrotron radiation (IRSR) is a powerful tool for microspectroscopy and imaging not only in the IR but also in the THz regions because of its high brilliance. Almost all IRSR beamlines in the world provide commercial IR microscopes end stations that are easy to use. Since Schwarzschild mirrors in commercial IR microscopes are small, the microscope is available only in the mid-IR region, *i.e.*, it is not suitable for the THz region. Then, we install a new microscope with large Schwarzschild mirrors in order to cover the IR region down to the THz region as shown in Fig. 3.

Some of the main features are; 1) Large working distance because some specific experiments (at very low temperatures, under high pressures, a near-field spectroscopy, etc.) are planned. 2) We need to cover the THz region because quasiparticle states of correlated materials and finger print vibration mode of proteins appear only in this spectral range. In order to achieve these goals, we use a large-size Schwarzschild mirrors (Diameter = 140 mm, NA = 0.5, working distance = 106 mm, magnification = $\times 8$) to reduce the diffraction effect in the THz region.

After installation of the THz microscope, we checked the spatial resolution in the different wavenumber ranges in which the microscope covers [7]. The THz microscope in conjunction with UVSOR-II covers down to 30 $\rm cm^{-1}$ in contrast that with a globar lamp covers above 500 $\rm cm^{-1}$. The spatial resolution and the intensity using UVSOR-II is much higher than that using a globar lamp in the whole wavenumber range. This indicates that the THz microscope using UVSOR-II is a very efficient means of microspectroscopy in the IR and THz regions.

We started the THz spectroscopy under high pressures. To detect the charge dynamics, the optical reflection spectroscopy [$R(\omega)$] in the THz region must be performed as mentioned in the previous section. The high pressure is produced by a diamond anvil cell. Since the sample area in the pressure cell is smaller than 1 mm in diameter, we have to use a microscopic technique. Then the THz spectroscopy under high pressures is difficult to perform using conventional FTIRs.

A membrane-type diamond anvil cell was employed to produce high pressures to samples. The schematic figure combined with THz microscope is shown in Fig 3. The pressure applied to samples is controlled by the helium gas pressure filled in the membrane. Since the areas of the culet plane of diamond and of the membrane are 1.13 $\rm mm^2$ and 1030 $\rm mm^2$, respectively, the pressure of samples is about 10^3 times larger than the helium gas pressure. The sample with a typical size of $0.4\times0.4\times0.05$ $\rm mm^3$ was set in a diamond anvil cell with Apiezon-N grease as the pressure medium and with a gold film as a reference and ruby tips as for a pressure reference. The pressure was calibrated by a ruby fluorescence measurement.

SmS is an insulator (it is called “black phase”) with the gap size of 1000 K at ambient pressure [16]. Above about 0.7 GPa, the sample color changes to gold (golden phase) and the Sm-ion changes from the divalence to mixed valence [17]. To investigate the mechanism of the transition, we performed the THz reflection spectroscopy under pressures.

The obtained $R(\omega)$ of SmS at 300 K as a function of pressure were shown by thick lines in Fig. 4(a). At the ambient pressure, the spectrum indicates the insulating character because the low energy limit does not approach to unity and a clear large peak due to the TO-phonon between Sm^{2+} and S^{2-} ions appears. When a pressure was applied, the background intensity increased with increasing pressure. The background indicates the appearance of carriers. Therefore the carrier density increases with increasing pressure. The fitting curve of the combi-

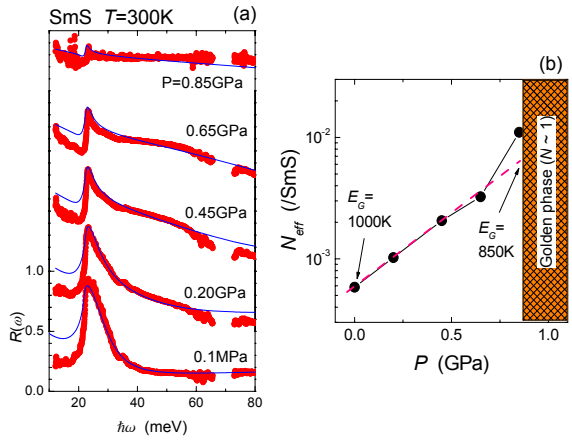

FIGURE 4. (a) Pressure dependence of reflectivity spectrum [$R(\omega)$] of SmS (thick lines) in the black phase at 300 K. The fitting curve of the combination of a Drude and a Lorentz functions are also plotted by thin solid lines. Successive curves are offset by 0.5 for clarity. (b) Pressure dependence of energy gap evaluated by the Drude and Lorentz fitting of $R(\omega)$ spectra. See the text for details.

nation of a Drude and a Lorentz functions is shown by thin solid lines in the same figure. The Lorentz function was set to reproduce the TO-phonon. To fit the obtained spectra, the N_{eff} in the Drude function is only changed and the other parameters (τ in the Drude function and all parameters in the Lorentz function) are fixed. The obtained N_{eff} is plotted in Fig. 4(b). The $\log N_{eff}$ is proportional to the pressure up to 0.65 GPa. The pressure dependence indicates that the energy gap closes with increasing pressure. The energy gap size (2Δ) at the ambient pressure was evaluated to be about 1000 K [16]. By evaluating the gap size from N_{eff}, the energy gap at the black-golden phase boundary is 850 K and then the gap suddenly closes to 100 K in the golden phase by the first order transition [18].

CONCLUSION

In conclusion, two examples of research activities of the terahertz spectroscopy and microspectroscopy at the infrared-terahertz beamline BL6B of UVSOR-II were reported. The performance of BL6B is excellent compared with a conventional globar light source. Some other experiments that cannot be performed by using conventional spectrometers, for instance, infrared magnetic circular dichroism [19], infrared reflection-absorption spectroscopy of adsorbed molecules on surfaces [7], subterahertz spectroscopy of superionic conductors and so on, are performed at the beamline. In the future, new terahertz spectroscopies will be produced at the beamline.

We would like to thank Prof. S. Kunii, Prof. N.K. Sato and Dr. K. Matsubayashi for their providing samples reported in this paper. This work was a joint study program of Institute for Molecular Science and was partially supported by Grants-in-Aid for Scientific Research (Grant No. 18340110) from MEXT of Japan and by the Research Foundation for Opto-Science and Technology.

REFERENCES

1. T. Nanba, Y. Urashima, M. Ikezawa, M. Watanabe, E. Nakamura, K. Fukui, and H. Inokuchi, *Int. J. Infrared and Millimeter Waves* **7**,1769 (1986).
2. M. Katoh, M. Hosaka, A. Mochihashi, J. Yamazami, K. Hayashi, Y. Hori, T. Honda, K. Haga, Y. Takashima, T. Koseki, S. Koda, H. Kitamura, T. Hara, and T. Tanaka, *AIP Conf. Proc.* **705**, 49 (2004).
3. S. Kimura, E. Nakamura, T. Nishi, Y. Sakurai, K. Hayashi, J. Yamazaki, and M. Katoh, *Infrared Sci. Tech.* **49**, 147 (2006).
4. S. Kimura, H. Kimura, T. Takahashi, K. Fukui, Y. Kondo, Y. Yoshimatsu, T. Moriwaki, T. Nanba, and T. Ishikawa, *Nucl. Instrum. Meth. A* **467-468**, 437 (2001).
5. S. Kimura, E. Nakamura, J. Yamazaki, M. Katoh, T. Nishi, H. Okamura, M. Matsunami, L. Chen, and T. Nanba, *AIP Conf. Proc.* **705**, 416 (2004).
6. S. Kimura, *Jpn. J. Appl. Phys.* **38** Suppl. 38-1, 392 (1999).
7. S. Kimura, Y. Sakurai, E. Nakamura, and T. Mizuno, *AIP Conf. Proc.* **879**, 595 (2006).
8. Y. Ikemoto, T. Moriwaki, T. Hirono, S. Kimura, K. Shinoda, M. Matsunami, N. Nagai, T. Nanba, K. Kobayashi, and H. Kimura, *Infrared Phys. Tech.* **45**, 369 (2004).
9. G. Travaglini and P. Wachter, *Phys. Rev. B* **29**, 893 (1984).
10. T. Nanba, H. Ohta, M. Motokawa, S. Kimura, S. Kunii, and T. Kasuya, *Physica B* **186-188**, 440 (1993).
11. S. Kimura, T. Nanba, S. Kunii, and T. Kasuya, *Phys. Rev. B* **50**, 1406 (1994).
12. G. Aeppli and Z. Fisk, *Comments Condens. Matter Phys.* **16**, 155 (1992).
13. T. Kasuya, K. Takegahara, Y. Aoki, K. Hanzawa, M. Kasaya, S. Kunii, T. Fujita, N. Sato, H. Kimura, T. Komatsubara, T. Furuno, and J. Rossat-Mignod, *Valence Fluctuation in Solids*, *p*. 215, (North-Holland, 1981).
14. P.A. Alekseev, J.M. Mignot, J. Rossat-Mignod, V.N. Lazukov, I.P. Sadikov, E.S. Konovalova, and Yu.B. Paderno, *J. Phys.: Condens. Matter* **7**, 289 (1995).
15. B. Gorchunov, N. Sluchanko, A. Volkov, M. Dressel, G. Knebel, A. Loidl, and S. Kunii, *Phys. Rev. B* **59**, 1808 (1999).
16. K. Matsubayashi, K. Imura, H.S. Suzuki, T. Mizuno, S. Kimura, T. Nishioka, K. Kodama, and N.K. Sato, *J. Phys. Soc. Jpn.* (2007) in press.
17. J.L. Kirk, K. Vedam, V. Narayanamurti, A. Jayaraman, and E. Bucher, *Phys. Rev. B* **6**, 3023 (1972).
18. T. Mizuno, S. Kimura, K. Matsubayashi, K. Imura, H.S. Suzuki, and N.K. Sato, submitted.
19. S. Kimura, M. Okuno, H. Iwata, H. Kitazawa, G. Kido, F. Ishiyama, and O. Sakai, *J. Phys. Soc. Jpn.* **71**, 2200 (2002).